Unknown Input Observer Based Detection of Sensor Faults in a Wind Turbine

Peter F. Odgaard, *Member, IEEE* and Jakob Stoustrup, *Senior Member IEEE*

***Abstract*—in this paper an unknown input observer is designed to detect a three different sensor fault scenarios in a specified bench mark model for fault detection and accommodation of wind turbines. In this paper a subset of faults is dealt with, it are faults in the rotor and generator speed sensors as well as a converter sensor fault. The proposed scheme detects the speed sensor faults in question within the specified requirements given in the bench mark model, while the converter fault is detected but not within the required time to detect.**

I. Introduction

As wind turbines increase in sizes and more wind turbine turbines are installed offshore, the need for fast fault detection and accommodation increases. In most industrial manufactured wind turbines only rather simplistic schemes are used to detect and accommodate faults.

A wind turbine converts wind energy to electrical energy. In this example a three blade horizontal axis turbine is considered. The blades are facing the wind direction; these blades are connected to the rotor shaft. The wind is moving the blades and thereby rotating the shaft. A gear box is used to upscale the rotational speed for the rotor in the generator and converter. In terms of control the turbine is working in two regions, partial and full power. In the partial power region the turbine is controlled to generate as much power as possible. This is obtained if a certain ratio between the tip speed of the blade and the wind speed is achieved. In this mode the converter torque is normally used to control the rotational speed of the rotor. In the second control mode the aerodynamics of the blades are controlled by pitching the blades.

In [7] a benchmark model of wind turbine with a number of different faults is presented, in which detection and accommodation requirements are as well defined. Among others it deals with faults in rotor and generator speed measurements as well as converter torque measurement.

Some examples can be found of fault detection and accommodation of wind turbines. An observer based scheme for detection of sensor faults for blade root torque sensors is presented in [11]. A residual based scheme is presented in [2] to detect and accommodate faults in wind turbines. Fault detection for electrical conversion systems can be found in [9, 10, 6] and [8]. In [3] an observer based scheme was proposed to detect and isolate sensor faults in the wind turbine drive train. An unknown input observer was used, to design an observer independent on the wind speed and thereby the aerodynamic torque acting on the wind turbine.

In this paper an unknown input observer is used as well, see [1]. Other examples on this usage of the unknown input observer can be seen in [5, 4] where the former reports this scheme applied on fault detection of power plant coal mills and the latter estimates power coefficients for wind turbines. An unknown input observer based scheme was in [3] proposed to detect such faults in a wind turbine. In which the wind turbine drive train is represented with a one body mass model, assuming a stiff drive train and as well now information of the wind speed. This model is in practice to simple. In this paper the observer design model is extended with a 2 body mass model of the drive train as specified in the bench mark model, see [7]. The observer in this paper is as well fed with the wind speed measurement assuming it being separated into a known and unknown part of which the known part corresponds to the measured one.

The wind turbine system is subsequently described in Section II, and in Section III the detection method is described, followed by a results section in Section IV and a conclusion in Section V.

II. System Description

The three blade horizontal axis turbine which is considered in this paper is controlled in the following way. In partial load, the wind turbine it is controlled to generate as much power as possible. This is achieved by keeping a specific ratio between the tip speed of the blades and the wind speed, which in turn is obtained by controlling the rotational speed through adjusting the converter torque. In the full power region the converter torque is kept constant and the rotational speed is adjusted by controlling the pitch angle of the blades which changes the aero-dynamical power transfer from wind to blades. This part of the wind turbine is illustrated in Fig. 1.

P.F. Odgaard is with kk-electronic a/s, 8260 Viby J, Denmark, (+45 21744963 peodg@kk-electronic.com).

J. Stoustrup is with Automation & Control, Department of Electronic Systems, Aalborg University, 9220 Aalborg East, Denmark, (Jakob@es.aau.dk)

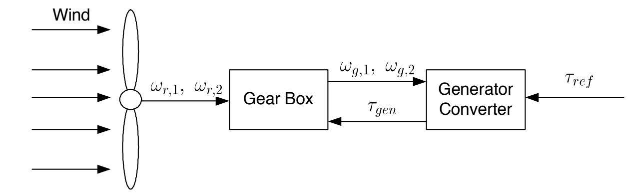

Fig. 1 Illustration of the principle of the wind turbine drive train. For illustrative purposes only two of the three blades are shown.

The wind turbine drive train in question has a number of measurements. $\omega_{r,1}[n]$ and $\omega_{r,2}[n]$ are two measurements of the rotor speed, $\omega_{g,1}[n]$ and $\omega_{g,2}[n]$ are two measurements of the generator speed, $\tau_{gen}[n]$ is the torque of the generator controlled by the converter which is provided with the torque reference, $\tau_{ref}[n]$. The estimated aerodynamic torque is defined as $\tau_{aero}[n]$. This estimate clearly depends on the wind speed, which unfortunately is very difficult to measure correctly. A very uncertain measurement is normally available which is used to provide 10 minutes mean values.

A. Model

The model is first defined in continuous time and subsequently transferred to discrete time.

The aerodynamic model is defined as in (1)

$$\tau_{\mathrm{aero}}(t) = \frac{\rho A C_{\mathrm{p}}(\theta(t), \lambda(t)) v^3(t)}{2\omega_{\mathrm{r}}(t)}, \qquad (1)$$

Where ρ is the density of the air, A is the area covered by the turbine blades in its rotation, $\theta(t)$ is the pitch angle of the blades, $\lambda(t)$ is the tip speed ratio of the blade. (1) is used to estimate $\tau_{\mathrm{aero}}(t)$ based on an assumed estimated $v(t)$ and measured $\theta(t)$ and $\omega_{\mathrm{r}}(t)$. Due to the uncertainty of the estimate this is separated into an estimated part, $\tilde{\tau}_{\mathrm{aero}}(t)$, and an unknown part, $\hat{\tau}_{\mathrm{aero}}(t)$, which means that

$$\tau_{\mathrm{aero}}(t) = \tilde{\tau}_{\mathrm{aero}}(t) + \hat{\tau}_{\mathrm{aero}}(t). \qquad (2)$$

In which $\tilde{\tau}_{\mathrm{aero}}(t)$ is computed using (1).

A simple one body model is used to represent the drive train, see (3).

$$J_r\dot{\omega}_r(t) = \tau_r(t) - K_{dt}\theta_\Delta(t) - (B_{dt} + B_r)\omega_r(t) + \frac{B_{dt}}{N_g}\omega_g(t), \qquad (3)$$

$$J_g\dot{\omega}_g(t) = \frac{\eta_{dt}K_{dt}}{N_g}\theta_\Delta(t) + \frac{\eta_{dt}B_{dt}}{N_g}\omega_g(t) - \left(\frac{\eta_{dt}B_{dt}}{N_g^2} + B_g\right)\omega_g(t) - \tau_g(t), \qquad (4)$$

$$\dot{\theta}_\Delta(t) = \omega_r(t) - \frac{1}{N_g}\omega_g(t), \qquad (5)$$

Where

$$\dot{\tau}_{gen}(t) = p_{gen}(\tau_{\mathrm{ref}}(t) - \tau_{\mathrm{gen}}(t)), \qquad (6)$$

J_r is the moment of inertia of the low speed shaft, K_{dt} is the torsion stiffness of the drive train, B_{dt} is the torsion damping coefficient of the drive train, B_g is the viscous friction of the high speed shaft, N_g is the gear ratio, J_g is the moment of inertia of the high speed shaft, η_{dt} is the efficiency of the drive train, and $\theta_\Delta(t)$ is the torsion angle of the drive train. The fault in terms of lower drive train efficiency is model by another parameter η_{dt2}. p_{gen} is the generator model parameter.

A state space model is given based on the bench mark model and it is subsequently discretized. This results in the following discrete time model.

$$\begin{bmatrix} \dot{\omega}_{\mathrm{r}}[n] \\ \dot{\omega}_{\mathrm{g}}[n] \\ \dot{\theta}_\Delta[n] \\ \dot{\tau}_{\mathrm{gen}}[n] \end{bmatrix} = \mathbf{A}_{\mathrm{d}} \begin{bmatrix} \omega_{\mathrm{r}}[n] \\ \omega_g[n] \\ \omega_\Delta[n] \\ \tau_{\mathrm{gen}}[n] \end{bmatrix} + \mathbf{B}_{\mathrm{d}} \begin{bmatrix} \tau_{\mathrm{ref}}[n] & \tilde{\tau}_{\mathrm{aero}}[n] \end{bmatrix} + \mathbf{E}_{\mathrm{d}} \begin{bmatrix} \hat{\tau}_{\mathrm{aero}}[n] & d[n] \end{bmatrix}, \qquad (7)$$

where $d[n]$ is unknown signal resulting in some robustness towards model uncertainties, and where

$$\mathbf{A}_{\mathrm{d}} = \begin{bmatrix} 0.8794 & 0.0013 & -0.5605 & -1.1326 \cdot 10^{-7} \\ 173.37 & -0.8256 & 800.11 & 1.187 \cdot 10^{-6} \\ 0.0114 & -1.192 \cdot 10^{-4} & -0.9456 & 4.313 \cdot 10^{-8} \\ 0 & 0 & 0 & 0.3679 \end{bmatrix}, \qquad (8)$$

$$\mathbf{B}_{\mathrm{d}} = \begin{bmatrix} 1.718 \cdot 10^{-9} & -3.470 \cdot 10^{-8} \\ 1.435 \cdot 10^{-7} & -4.427 \cdot 10^{-5} \\ 4.467 \cdot 10^{-11} & 2.307 \cdot 10^{-8} \\ 0 & 0.6321 \end{bmatrix}, \qquad (9)$$

$$\mathbf{E}_{\mathrm{d}} = \begin{bmatrix} 0.8246 & -1.206 \\ 252.3 & 1734 \\ 0.036 & 0.1139 \\ 0.0063 & 0.0632 \end{bmatrix}. \qquad (10)$$

The output equation is:

$$\begin{bmatrix} \omega_{r,1}[n] \\ \omega_{r,2}[n] \\ \omega_{g,1}[n] \\ \omega_{g,2}[n] \\ \tau_{\mathrm{gen}}[n] \end{bmatrix} = \begin{bmatrix} 1 & 0 & 0 & 0 \\ 1 & 0 & 0 & 0 \\ 0 & 1 & 0 & 0 \\ 0 & 1 & 0 & 0 \\ 0 & 0 & 0 & 1 \end{bmatrix} \begin{bmatrix} \omega_r[n] \\ \omega_g[n] \\ \omega_\Delta[n] \\ \tau_{gen}[n] \end{bmatrix}, \qquad (11)$$

III. METHOD

Due to the uncertainty of the estimation of τ_{aero} it would be preferable to introduce some robustness in the fault detection scheme. One could see the uncertainty as an unknown input signal; consequently an unknown input observer is an obvious choice, see [1]. If system is of the following form

$$\mathbf{x}[n+1] = \mathbf{A}\mathbf{x}[n] + \mathbf{B}\mathbf{u}[n] + \mathbf{E}d[n], \qquad (12)$$

$$\mathbf{y}[n] = \mathbf{C}\mathbf{x}[n], \qquad (13)$$

where $d[n]$ is an unknown input, and $\mathbf{E}$ is the unknown input matrix.

The unknown input observer can be found as in (14)-(15).

$$\mathbf{z}[n+1] = \mathbf{F}_{n+1}\mathbf{z}[n] + \mathbf{T}_{n+1}\mathbf{B}_n\mathbf{u}[n] + \mathbf{K}_{n+1}\mathbf{y}[n], \qquad (14)$$

$$\hat{\mathbf{x}}[n+1] = \mathbf{z}[n+1] + \mathbf{H}_{n+1}\mathbf{y}[n+1], \qquad (15)$$

where $\mathbf{F}_{n+1},\ \mathbf{T}_{n+1},\ \mathbf{K}_{n+1}$ and $\mathbf{H}_{n+1}$are matrices designed to achieve decoupling from the unknown input and as well obtain an optimal observer. $\hat{x}$ is a vector of the states of the wind turbine model. The matrices in the unknown input observer are found using the following equation see (16)-(23), since system matrices are assumed constant these observer matrices are constant as well.

$$\mathbf{H} = \mathbf{E}(\mathbf{C}\mathbf{E})^+, \qquad (16)$$

$$\mathbf{T} = \mathbf{I} + \mathbf{H}\mathbf{C}, \qquad (17)$$

$$\mathbf{F} = \mathbf{A} - \mathbf{H}\mathbf{C}\mathbf{A} - \mathbf{K}^1\mathbf{C}, \qquad (18)$$

$$\mathbf{K}^2 = \mathbf{F}\mathbf{H}, \qquad (19)$$

$$\mathbf{K}^1 = \mathbf{A}^1\mathbf{P}\mathbf{C}^T\left(\mathbf{C}\mathbf{P}\mathbf{C}^T + \mathbf{R}\right)^{-1}, \quad (20)$$
$$\mathbf{A}^1 = \mathbf{A} - \mathbf{HCA}, \quad (21)$$
$$\mathbf{P} = \mathbf{A}^1\mathbf{P}^1(\mathbf{A}^1)^T + \mathbf{TQT}^T + \mathbf{HRH}^T, \quad (22)$$
$$\mathbf{P}^1 = \mathbf{P} - \mathbf{K}^1\mathbf{CP}(\mathbf{A}^1)^T, \quad (23)$$

The system states can subsequently be estimated by (14)-(15).

A. Residual generation

In order to generate the residuals for the fault detection and isolation system a residual $\mathbf{r}^i$ is computed for each sensor i using the unknown input observer scheme for a model where the ith sensor is removed from the C matrix and measurements, and define this matrix as $\mathbf{C}^i$, and the measurement vector from which the ith is removed is defined as $\mathbf{y}^i$. The observer for estimating $\mathbf{r}^i$ can be seen in (24)-(25).

$$\mathbf{z}[n+1] = \mathbf{F}^i\mathbf{z}^i[n] + \mathbf{T}^i\mathbf{B}\mathbf{u}[n] + \mathbf{K}^i\mathbf{y}^i[n], \quad (24)$$
$$\mathbf{r}^i[n] = (\mathbf{I} - \mathbf{C}^i\mathbf{H}^i\mathbf{y}^i[n] - \mathbf{C}^i\mathbf{z}^i[n], \quad (25)$$

The matrices $\mathbf{F}^i$, $\mathbf{T}^i$, $\mathbf{K}^i$, $\mathbf{H}^i$, are found as in (16)-(23) with the only difference that $\mathbf{C}$ is replaced with $\mathbf{C}^i$. The residual vector consists of some elements defined as, in this case with 5 sensors

$$\mathbf{r}^i[n] = \begin{bmatrix} r_1^1 \\ r_2^i \\ r_3^i \\ r_4^i \end{bmatrix}, \quad (26)$$

These computed residuals are subsequently used to compute the actual detection signal. Define the detection signal for the five sensors as: $\kappa_{\omega_{r,1}}$, $\kappa_{\omega_{r,2}}$ as the two rotor angular speed detection signals, $\kappa_{\omega_{g,1}}$, $\kappa_{\omega_{g,2}}$, and κ_{τ_g} as the generator torque detection signal. These detection signals are computed as in (27)-(31).

$$\kappa_{\omega_{r,1}}[n] = r_1^2[n] \cdot r_1^3[n] \cdot r_1^4[n] \cdot r_1^5[n], \quad (27)$$
$$\kappa_{\omega_{r,2}}[n] = r_1^1[n] \cdot r_2^3[n] \cdot r_2^4[n] \cdot r_2^5[n], \quad (28)$$
$$\kappa_{\omega_{g,1}}[n] = r_2^1[n] \cdot r_2^2[n] \cdot r_3^4[n] \cdot r_3^5[n], \quad (29)$$
$$\kappa_{\omega_{g,2}}[n] = r_3^1[n] \cdot r_3^2[n] \cdot r_3^3[n] \cdot r_4^5[n], \quad (30)$$
$$\kappa_{\tau_g}[n] = r_4^1[n] \cdot r_4^2[n] \cdot r_4^3[n] \cdot r_4^4[n], \quad (31)$$

A sensor fault is present at the ith sensor if

$$|\kappa_i[n]| > \gamma_i \cdot \kappa_i^{\max}, \quad (32)$$

Where γ_i is the threshold of the ith fault residual, and $\kappa_i^{\max}$ is the recorded maximal value of the κ_i. The values of these thresholds are found tests on the simulated data, such that false positive detections are avoided while the sensor fault is still detected as fast as possible. The values are specified as:

$$\gamma_1 = 0.15,\ \gamma_2 = 0.15,\ \gamma_3 = 0.15,\ \gamma_4 = 0.15,\ \gamma_5 = 0.15$$

IV. Results

In this paper only 3 of the faults from the faults from the bench mark model, see [7], are dealt with. In the bench mark model a number of faults in different parts of a wind turbine is included.

In this paper only fault # 4, 5 & 8 are detected, which respectively are: a fixed valued on rotor speed measurement number 1 from 1500-1600 seconds (the value equal 1.4), a gain error on rotor speed measurement no 2 and generator speed measurement no. 1 with respectively a gain factor on 1.1 and 0.9 from 1000-1100 seconds, and an offset on the converter/generator torque with the value of 100 from 3800-3900 seconds. In case of the speed sensors the beginning and end of these faults should be detected with in 0.1 seconds due to the bench mark requirements, and in case of the converter fault the beginning and end of the fault should be detected within 0.03 seconds, see [7].

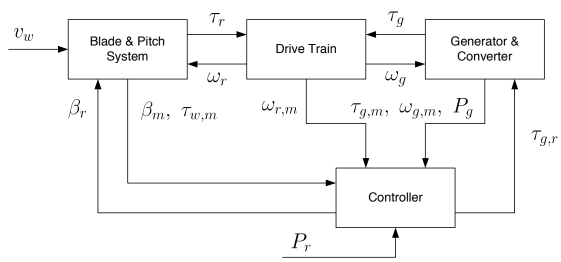

Fig. 2 A graphical overview of the simulation model given by the bench mark model.

A graphical overview of the bench mark model can be seen in Fig. 2 in which P_r is the power reference, P_g is the generator power, β_r, is the pitch reference and β_m is the pitch position measurements.

The simulation is performed with a wind input sequence defined in the bench mark model, see Fig. 3.

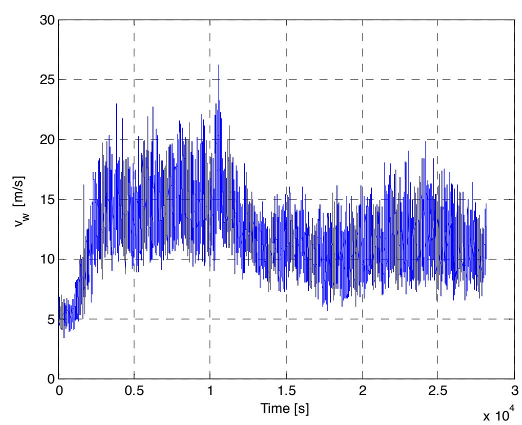

Fig. 3 Wind speed input sequence used in the bench mark simulation model.

A. Fault 4

Detection of this fault can be seen from a plot of the residual corresponding to $\omega_{r,m1}[n]$, which can be seen in Fig. 4 from which it can be seen that there is a clear detection of the fault during it occurrence even though that some reactions on fault 5 is present, however, it is still below the thresh hold. A zoom on the beginning and end of the detection are plotted in Fig. 5.

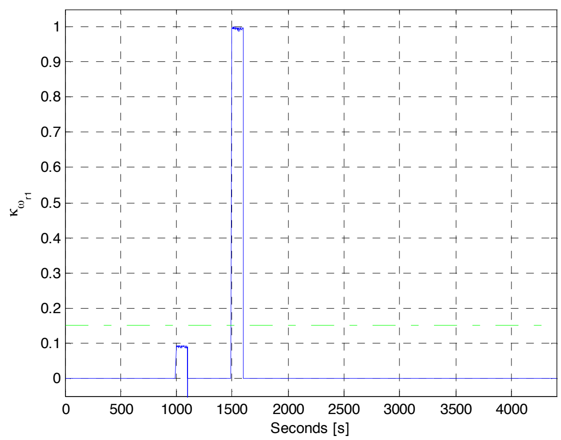

Fig. 4 The plot of the residual $\kappa_{\omega_{r,1}}[n]$.

From this plot it can be seen that the beginning and end of the fault is detected with in 0.1 seconds corresponding to 10 times the used sample time.

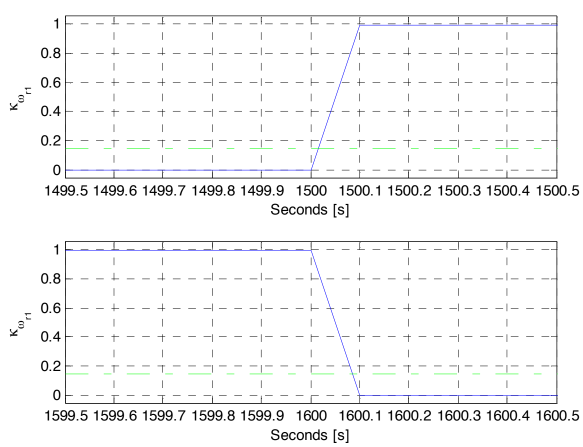

Fig. 5 A zoom on the beginning and end of the residual $\kappa_{\omega_{r,1}}[n]$.

B. Fault 5

Fault number 5 corresponds to gain factor on $\omega_{r,m2}[n]$ with a factor of 1.1 and on $\omega_{g,m1}[n]$ with a factor of 0.9 in the time interval between 1000 and 1100 seconds.

A plot of the residual $\kappa_{\omega_{r,2}}[n]$ can be seen in Fig. 6, from which it can be seen that fault number 5 is detected without any false positive detections of the other faults.

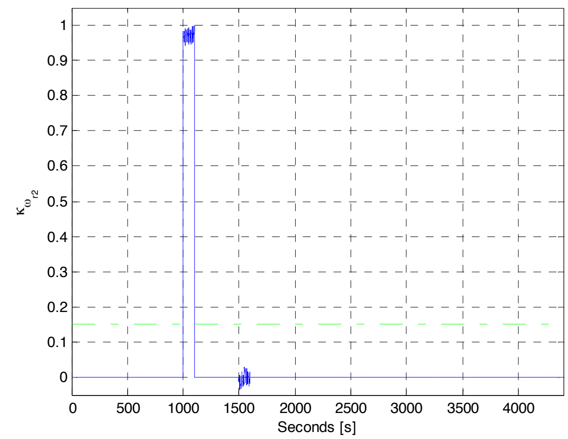

Fig. 6 The plot of residual $\kappa_{\omega_{r,2}}[n]$.

The timings of the beginning and ends of the fault detection of $\omega_{r,m2}[n]$ can be seen from a zoom on Fig. 6, which can be seen in Fig. 7. From this plot it can be seen that the fault is detected with 0.1 seconds both in terms of beginning detection and end detection.

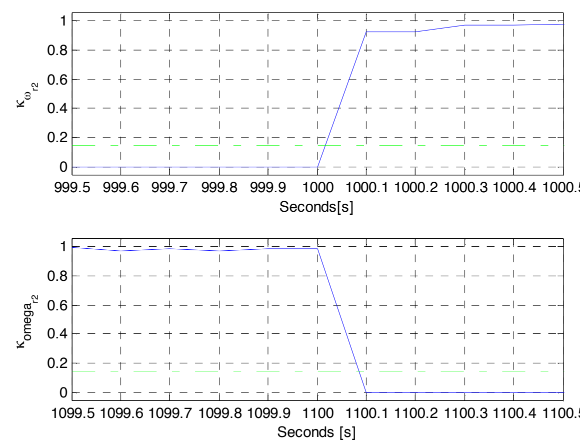

Fig. 7 A zoom on the beginning and end of the residual $\kappa_{\omega_{r,2}}[n]$.

The residual $\kappa_{\omega_{g,1}}[n]$ is plotted in Fig. 8, which clearly indicates a detection of the fault and no clear response to the other faults.

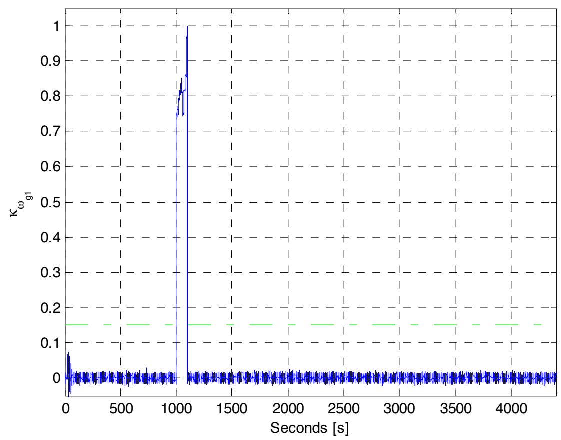

Fig. 8 A plot of the residual $\kappa_{\omega_{g,1}}[n]$.

A zoom on the beginning and end of the fault in the residual $\kappa_{\omega_{g,1}}[n]$ can be seen in Fig. 9, from which it can be seen that this fault is detected within the required 0.1 second both in terms of detection of the beginning and the end.

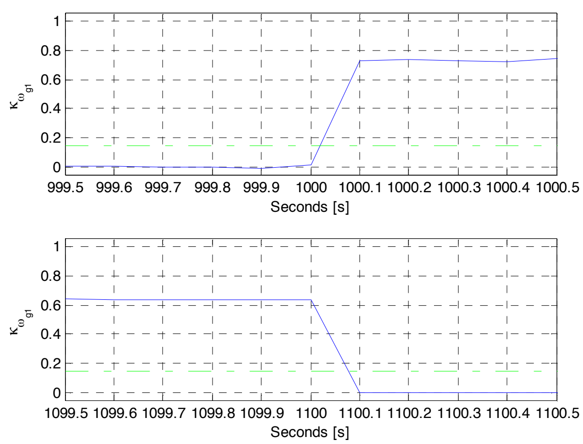

Fig. 9 A zoom on the beginning and end of the residual $\kappa_{\omega_{g,1}}[n]$.

C. *Fault 8*

This fault corresponds to an offset on the converter torque measurement/estimate on 100 Nm from 3800s-3900s. The residual corresponding to this fault can be seen in Fig. 10.

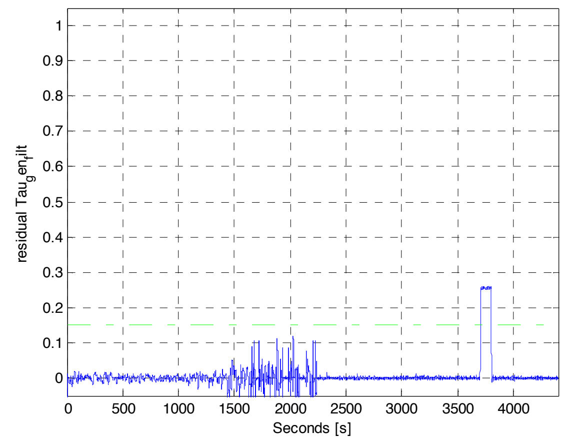

Fig. 10 The residual $\kappa_{\tau_g}[n]$

It can be seen that the fault is detected, while some influence on the residual is due other faults than the ones mentioned in this paper, see [7]. A zoom on the detections beginning and ends can be seen in Fig. 11, from which it can be seen that the fault is not detected with 0.03 seconds. The beginning detection is detected at 0.05 seconds and the end at 0.08 seconds.

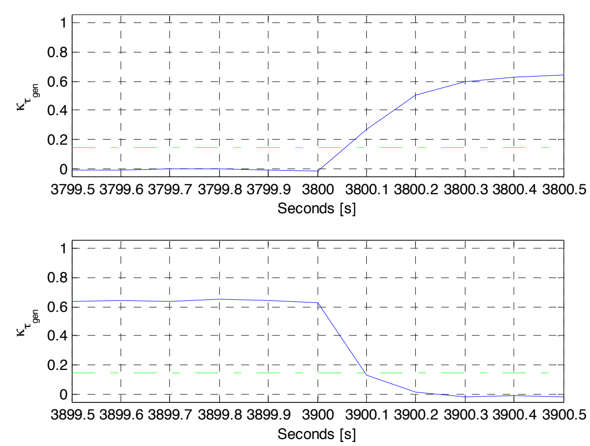

Fig. 11 A zoom on the beginning and end of the residual $\kappa_{\tau_g}[n]$.

D. *Summary of fault detection simulations*

The two speed sensor faults were all detected within the requirements presented in the bench mark model requirements. On the other hand the proposed scheme could not detect the converter fault within the requirement, which in the case of converter faults is set to 0.03 seconds, and the beginning was detected at 0.05 seconds and the end at 0.08 seconds. In this paper only one simulation of the fault and detection is presented, it has, however, been verified with Monte Carlo simulations (100 simulations), that the detection delays are in all cases as shown in the examples in the paper. Consequently it can be concluded that the proposed scheme was not fast enough to detect the fault in the converter.

V. Conclusions

In this paper an unknown input observer based scheme is applied to some sensor faults presented in bench mark model of fault detection and accommodation of wind turbine faults. In this paper the two different speed sensor faults are detected within the detection requirements specified by the bench mark model, while the converter fault is detected but not within the required time.

References

[1] Jie Chen and R. J. Patton. *Robust model-based fault diagnosis for dynamic systems*. Kluwer academic publishers, first edition, 1999.

[2] C. Dobrila and R. Stefansen. Fault tolerant wind turbine control. Master's thesis, Technical University of Denmark, Kgl. Lyngby, Denmark, 2007.

[3] P. F. Odgaard, J. Stoustrup, R. Nielsen, and C. Damgaard. Observer based detection of sensor faults in wind turbines. In *Proceedings of European Wind Energy Conference 2009*, Marseille, France, March 2009. EWEA, EWEA.

[4] P.F. Odgaard, C. Damgaard, and R. Nielsen. On-line estimation of wind turbine power coefficients using unknown input observers. In *Proceedings of the 17th World Congress The International Federation of Automatic Control*, pages 10646–10651, Seoul, Korea, July 2008. IFAC, IFAC.

[5] P.F. Odgaard and B. Mataji. Observer based fault detection and moisture estimating in coal mill. *Control Engineering Practice*, 16(8):909–921, August 2008.

[6] P.F. Odgaard and J. Stoustrup. Unknown input observer based scheme for detecting faults in a wind turbine converter. In *Proceedings of the 7th IFAC Symposium on Fault Detection, Supervision and Safety of Technical Processes*, pages 161–166, Barcelona, Spain, June-July 2009. IFAC.

[7] P.F. Odgaard, J. Stoustrup, and M. Kinnaert. Fault tolerant control of wind turbines - a benchmark model. In *Proceedings of the 7th IFAC Symposium on Fault Detection, Supervision and Safety of Technical Processes*, pages 155–160, Barcelona, Spain, June-July 2009. IFAC.

[8] P. Poure, P. Weber, D. Theilliol, and S. Saadate. Fault-tolerant power electronic converters: Reliability analysis of active power filter. In P. Weber, editor, *Proc. IEEE International Symposium on Industrial Electronics ISIE 2007*, pages 3174–3179, 2007.

[9] K. Rothenhagen and F.W. Fuchs. Current sensor fault detection and reconfiguration for a doubly fed induction generator. In F.W. Fuchs, editor, *Proc. IEEE Power Electronics Specialists Conference PESC 2007*, pages 2732–2738, 2007.

[10] K. Rothenhagen, S. Thomsen, and F.W. Fuchs. Voltage sensor fault detection and reconfiguration for a doubly fed induction generator. In S. Thomsen, editor, *Proc. IEEE International Symposium on Diagnostics for Electric Machines, Power Electronics and Drives SDEMPED 2007*, pages 377–382, 2007.

[11] X. Wei, M. Verhaegen, and T. van den Engelen. Sensor fault diagnosis of wind turbines for fault tolerant. In *Proceedings of the 17th World Congress The International Federation of Automatic Control*, pages 3222–3227, Seoul, South Korea, July 2008. IFAC.